Expression of the *HSF4 DNA Binding Domain-EGFP* Hybrid Gene Recreates Early Childhood Lamellar Cataract in Transgenic Mice

Rajendra K. Gangalum,[1] Zhe Jing,[1] Ankur M. Bhat,[1] Josh Lee, Yoshiko Nagaoka,[2] Sophie X. Deng,[3] Meisheng Jiang,[2] and Suraj P. Bhat[1,3]

[1]Jules Stein Eye Institute, Geffen School of Medicine at University of California Los Angeles, Los Angeles, California, United States
[2]Department of Molecular and Medical Pharmacology, Geffen School of Medicine at University of California Los Angeles, Los Angeles, California, United States
[3]Molecular Biology Institute and Brain Research Institute, University of California Los Angeles, Los Angeles, California, United States

Correspondence: Suraj P. Bhat, 100 Stein Plaza, BH263, Geffen School of Medicine at UCLA, Los Angeles, CA 90095, USA; bhat@jsei.ucla.edu.

RKG and ZJ contributed equally to the work presented here and should therefore be regarded as equivalent authors.

Submitted: April 14, 2014
Accepted: August 8, 2014

Citation: Gangalum RK, Jing Z, Bhat AM, et al. Expression of the *HSF4 DNA binding domain-EGFP* hybrid gene recreates early childhood lamellar cataract in transgenic mice. *Invest Ophthalmol Vis Sci*. 2014;55:7227–7240. DOI:10.1167/iovs.14-14594

Purpose The clinical management of cataracts in infancy involves surgical removal of the lens to ensure transmission of light to the retina, which is essential for normal neural development of the infant**.** This surgery, however, entails a lifelong follow-up and impaired vision. To our knowledge, no animal models recapitulate human lamellar opacities, the most prevalent form of early childhood cataracts. We present data on the recreation of the human lamellar cataract phenotype in transgenic mice.

Methods. Mutations in the DNA binding domain (DBD) of the heat shock transcription factor 4 (HSF4) are known to be associated with early childhood autosomal dominant lamellar cataract. We used bacterial artificial chromosome (BAC) transgenesis to express a hybrid gene: *Hsf4* (DBD)–enhanced green fluorescent protein (*EGFP*), by recombineering EGFP sequences into the DBD of the *Hsf4* gene, to interfere with the DNA binding properties of Hsf4.

Results. We recapitulated the human lamellar cataract, in its temporal as well as spatial presentation, within the transgenic mouse lens. This phenotype was reproduced faithfully using four different BACs, indicating that EGFP can be used to target transcription factor function in transgenic mice. Molecular and cell biological examination of early postnatal transgenic lens reveals impairment of secondary fiber cell differentiation.

Conclusions. Recreation of the human lamellar cataract phenotype in mice allows investigation of this human pathology at a level not possible previously and points to the relevance of fiber cell heterogeneity dictated by fiber cell–specific gene activity in the biogenesis of the lamellar cataract.

Keywords: lens, cataract, transgenic mice, *HSF4*, BACs

Cataract or opacification of the eye lens impedes transmission of light to the retina. Light deprivation of the developing eye in early childhood or infancy, however, has grave consequences for the development of the brain. To allow normal neural development, in infants, the cataract may be removed as early as two months of age, but the children may suffer from impaired vision for the rest of their lives.[1] The consequences of cataract surgeries in children, particularly in their infancy, are calamitous; up to two-thirds (estimates are 32%–59%) of these children suffer from glaucoma (degeneration of retinal ganglion cells) that leads to eventual blindness.[1–4]

Congenital cataracts make approximately 10% of early childhood cataracts. Approximately half of all congenital cataracts are inherited.[5,6] Among these, the lamellar cataract, a bilateral condition, is the most prevalent form of childhood cataracts.[7,8] As the name would suggest, the cataract is confined to a single lamella (or layer) in the area between the primary and secondary fiber cell morphogenesis in the developing ocular lens. The cataract may not cover a whole layer of fiber cells; it also may be represented by dots or points of opacity within the fetal nucleus. This cataract also has been called the perinuclear, zonular, and Marner's cataract.[9,10]

The human lamellar cataract appears at a specific developmental time in the context of the morphogenesis of the lens, which is attended by regional demarcations that are temporally and developmentally distinguishable. The "embryonic nucleus" of the ocular lens is derived from primary fiber cell differentiation, while the fetal nucleus and adult cortex are generated by the differentiation of the secondary fiber cells (see the review of Bhat[11]). In the lamellar cataract, typically a clear embryonic nucleus and a clear cortex are interrupted by a cataractous layer of fiber cells. Thus, unlike complete nuclear or whole cortex cataracts, the lamellar cataract is confined morphologically. However, to our knowledge, no paradigms are available for the study of these most prevalent childhood lens cataracts.

A number of animal models are available for the study of developmental and/or genetically predisposed cataracts, including mutagen-induced mouse models,[12] while others have been produced in the transgenic mice with the expression of foreign gene sequences in the lens.[13–16] Many of the transgenic

Copyright 2014 The Association for Research in Vision and Ophthalmology, Inc.

paradigms produce gross morphologic changes, which makes it difficult to investigate the initiating event(s). This may be because of the unregulated expression from a heterologous and/or small promoter sequence (such as the use of the promoter of *αA-crystallin* gene, commonly used for directing transgenes to the lens), which may not regulate the transgene correctly, temporally, or spatially. Mutations known in human genes for lens structural proteins also have been introduced into transgenic mice,[17] but the interpretations of the data remain complicated by the inability to separate phenotype(s) due to unknown catalytic properties of the crystallins from their structural/refractive functions.[18–21]

Mutations in heat shock transcription factor 4 (HSF4) have been associated with autosomal dominant as well as recessive cataracts.[22–25] The human lamellar cataract has been associated with missense autosomal dominant mutations in the DNA binding domain (DBD) of HSF4,[26,27] which is one of the four heat shock factors (HSFs) in the eukaryotic cell.[28] The HSF4, the focus of this study, is a constitutively trimeric transcription factor, which is present in the cytoplasm as well as the nucleus. It does not respond to the heat shock as robustly as does the HSF1.[28] Its expression is developmentally controlled and, importantly, the appearance of the lamellar cataract in early childhood follows its predominantly postnatal expression.[29–32] It is obvious that the morphologically confined lamellar cataract arises because of differential gene activity modulated by the mutant transcription factor Hsf4 in a subset of fibers (or lamellae).

The HSFs are highly homologous proteins.[33] The mouse (Accession #NP_001242971.1) and human (Accession #NP_001035757.1) HSF4 proteins share up to 90% identities at the amino acid level; in the DBD they are identical (18–122 amino acids). Notably, most of the mutations in the DBD are associated with discreet lamellar cataracts,[26,27] while recessive mutations, which morphologically involve most of the lens, usually are seen in the C-terminus half of the protein.[24,25] Based on these observations, we selected exon 1 (that codes for the N-terminus of the HSF4 protein, including 23 residues of the DBD), as the N-terminus of a hybrid gene product, that would interfere with the DNA binding activity of the endogenous HSF4, when expressed as a transgene in the developing lens. The motivation is to recapitulate the confined phenotype wherein most of the lens would be "normal," a characteristic of the lamellar cataract phenotype associated with mutations in the DBD in the very N-terminus of the HSF4 protein. We hypothesized that interference with *Hsf4* directed gene activity at a specific time and within specific lamellae (fiber cells) in the developing transgenic mouse lens should reproduce this pathology.

Methods

All animal experiments were performed according to the guidelines of the Animal Research Committee, Division of Laboratory Animal Medicine, University of California, Los Angeles (UCLA), and the Association for Research in Vision and Ophthalmology (ARVO) Statement for the Use of Animals in Ophthalmic and Vision Research.

Bacterial Artificial Chromosome (BAC) Recombineering

The BAC clones containing the *Hsf4* gene were purchased from Children's Hospital Oakland Research Institute (CHORI; Oakland, CA, USA). Four BAC DNAs of various lengths (RP23-203H14, BAC #1, 220 kb; RP23-118P12, BAC #4, 228 kb; RP24-227N21 BAC #7, 170 kb, and RP24-131O24, BAC #8, 160 Kb) were labeled as N1, N4, N7, and N8. The BAC DNAs were maintained in *Escherichia coli* DH10B and then used for the manipulation of the *Hsf4* gene through recombineering (Figs. 1, 2).

Construction of the Vector Plasmid

The DBD (104 amino acids long) of Hsf4 protein is encoded by the first four exons of the *Hsf4* gene (Fig. 2B). We inserted enhanced green fluorescent protein (EGFP) sequences at the end of the exon1 such that a hybrid gene transcript (*Hsf4* [exon1] DBD-*EGFP*-PolyA) is produced when the *Hsf4* transgene from the BACs is expressed. To modify the *Hsf4* sequences within the BACs, a vector plasmid, pBSK-EGFP - FRT1-Tn5-neo-FRT2 (Gene Bridges GmBH, Heidelberg, Germany) that would carry the intended manipulation into the *Hsf4* gene was modified in our laboratory. A stop codon was added at the end of the EGFP coding sequence followed by two SV40 PolyA signals, AATAAAAATAAA stretches, upstream of FRT-Tn5-neo-FRT cassette to terminate the translation of the mRNA from the hybrid gene effectively.

Preparation of the Targeting Cassette

The linear targeting cassette containing the EGFP-PolyA- FRT-Tn5-neo-FRT cassette was generated from the modified plasmid, pBSK–EGFP-PolyA-PolyA-FRT1-Tn5-neo-FRT2 (Gene Bridges GmBH) by PCR using the following primers: (forward primer [F], 5′-GGGCGCTGGTAGGCGACCCAGGCACCGACCACCTCATCCGCTGGAGCCCGATGGTGAGCAAGGGCGAGGAGCT-3′; reverse [R], 5′- TGGAGGGATCCCGGGGACCACTGAAGGAGTTGAG GGGCCCCAGCCCTCACGAAGTTCCTATACTTTCTAGAGAA-3′). This targeting fragment, thus, contains 50 base pairs (bp) each of left homologous arm (LHA) and right homologous arm (RHA; underlined sequences in the oligos), respectively. These sequences were derived from the 5′exonic sequence and from the 3′intronic sequence at the end of exon1 (of the *Hsf4* gene), the point of insertion. The linear PCR product, the targeting cassette (LHA-EGFP-PolyA-PolyA-FRT-Tn5-neo-FRT-RHA), was sequenced and gel purified (Fig. 1, Step 4, Gel 1) before BAC recombineering.[34]

Recombineering EGFP Into *Hsf4* Gene in Various BACs

The cells containing the BAC and recombinase proteins (RecE and RecT from pRed/ET plasmid) were transfected with 1 μg of purified linear targeting cassette fragment. The Chl^r and Kan^r colonies were grown, and the integration of the LHA-EGFP-PolyA-PolyA-FRT-Tn5-neo-FRT-RHA in the BAC was confirmed by colony PCR for the recombinant clones (forward primer, 5′-TTCAAGGACGACGGCAACTA-3′; and reverse primer, 5′-TAAGTTCCTATACTTTCTCGAGAA-3′; Fig. 1, Gel 2, 1490 bp amplicon). The recombineered BAC DNA with the targeting cassette (Hsf4-EGFP-PolyA-PolyA-FRT-Tn5-neo-FRT) was purified and retransformed into fresh DH10B *E. coli* (Chl^r/Kan^r). These clones then were transformed with p707FLPe (Tet^r plasmid, which carries thermosensitive CI578 λ_{PR} promoter). The cultures were grown at 30°C for 3 hours and then at 38.5°C for 15 hours to resolve the TN5-neo-FRT cassette, the p707FLPe is lost at this temperature. The resolved and unresolved clones were identified by colony PCR (forward primer, 5′-CAGAGAAAGAGAGGCACTCG-3′ and reverse primer, 5′-TGGAGGGACCCGGGGACCAC-3′; Fig. 1, Gel 3). The final Hsf4-EGFP-PolyA-PolyA-FRT BAC DNA was sequenced across the recombination region to confirm correct insertion.

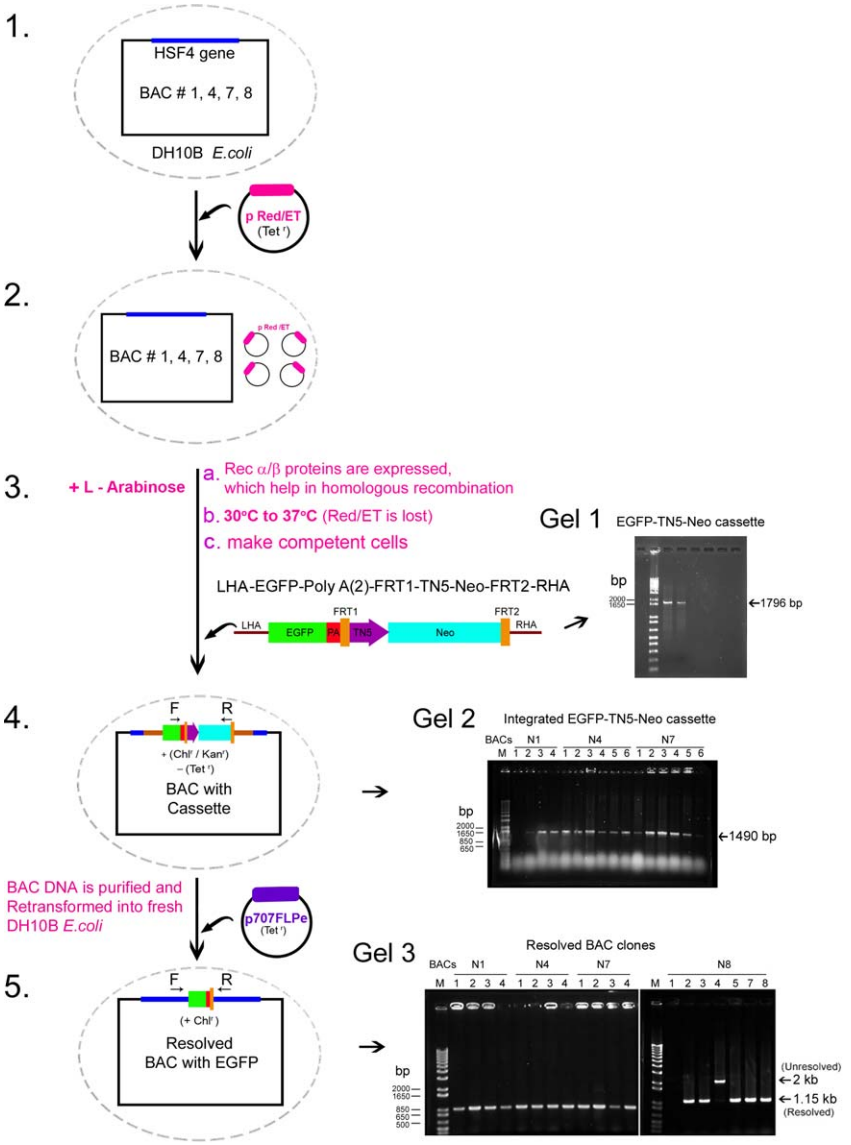

Figure 1. Recombineering EGFP into the DNA binding domain of the *Hsf4* gene in various BACs. (**1**) Four mouse BACs (mHsf4 BAC # N1, N4, N7, and N8) of various lengths (see Fig. 2), containing the *Hsf4* gene were maintained in *E. coli* strain DH10B. (**2**) The pRed/ET plasmid Tet^r[59] was transformed into *E. coli* harboring Hsf4-BAC DNA. (**3**) The recombinase functions (Rec α/ Rec β proteins) from this plasmid were induced by L-arabinose (10%) overnight and the culture was shifted to 37°C that inhibits the replication of the plasmid. The cultures were selected on Chl^r/Tet^s plates and transformed with the purified linear targeting cassette DNA fragment (LHA-EGFP-PolyA-PolyA-FRT1-Tn5-neo-FRT2-RHA) (Gel 1). (**4**) The Chl^r and Kan^r colonies were grown and screened by colony PCR (1490 bp amplicon) (Gel 2). (**5**) The recombineered BAC DNA with the targeting cassette (Hsf4-EGFP-PolyA-PolyA-FRT1-Tn5-neo-FRT2) was purified and retransformed into fresh DH10B *E.coli* (Chl^r/Kan^r) and then transformed with p707FLPe. The FLP expression, which is repressed at 30°C was induced at 38.5°C to resolve the TN5-neo-FRT cassette, the p707FLPe is lost at this temperature. The resolved and unresolved clones were identified by colony PCR: unresolved (2 kb amplicon) and resolved (1.15 kb amplicon) (Gel 3). Finally, the resolved BAC DNA with EGFP-PolyA was purified and injected into the pronuclei of 0.5 day, one cell–staged embryos (C57Blk6) for generating the transgenic mice.[34]

Generation and Maintenance of Transgenic Mice

The modified BAC DNAs were purified using RECOCHIP cassettes[34] and microinjected into C57Blk6 pronuclear stage embryos to generate transgenic mice. The efficiency of the generation of the transgenics with manipulated BACs was between 63% and 83.3%.[34] The lamellar cataract phenotype was detected (by slit-lamp examination) in all founders (69 in all). Of these founders, 40% were used for morphologic characterization (hematoxylin and eosin [H&E] and light microscopy) and 60% for breeding. Founders were crossed with age-matched wild type mice (C57Blk6) to produce F1 progeny. The F1 mice (~4 mouse lines/BAC) then were inbred (brother–sister mating) to generate the F2 progeny. The F2 mice (5 mouse lines/BAC) were inbred for five generations for each BAC.

Slit-Lamp Ophthalmoscopy

Transgenic mice were examined by a slit-lamp ophthalmoscope (BM900; Hagg-Streit, Bern, Switzerland) modified in our laboratory with an Accu beam II connector and detachable Cannon camera (EOS Rebel T2i; Canon, Tokyo, Japan) and fitted with a platform for the examination of the live, nonanesthetized

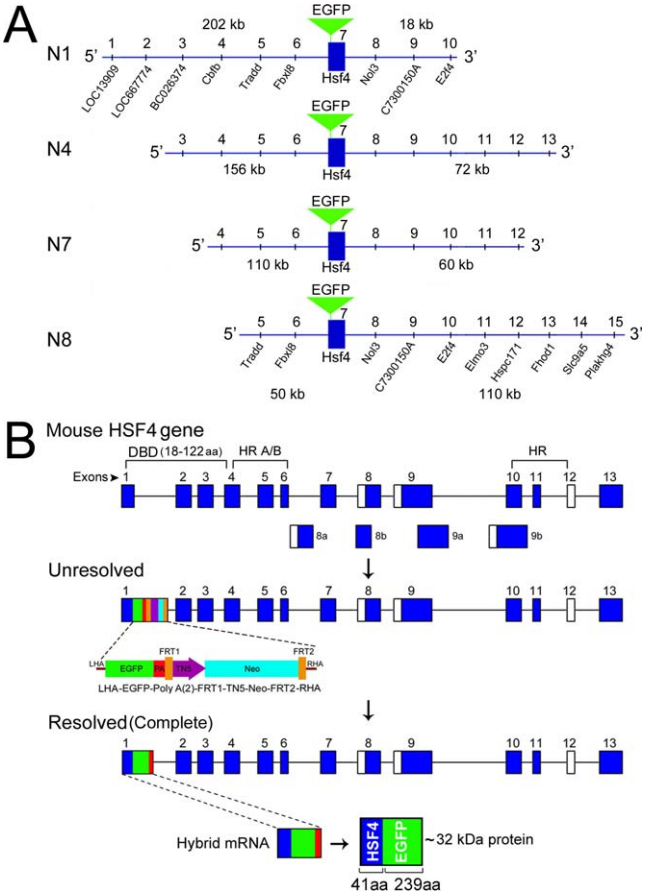

Figure 2. The *Hsf4* manipulated sequences within mouse BACs for expression in the developing ocular lens. (**A**) N1, N4, N7, and N8 represent four BACs with different lengths of the 5′ (202–50 kb) and 3′ (18–110 kb) surrounding the *Hsf4* gene. The common location of the EGFP (*green inverted triangle*) in the DNA binding domain, at the end of exon 1 of the *Hsf4* gene is shown. The markings *1* to *10* designate the positions of the known genes (UCSC Genome Browser). (**B**) The first schematic shows the *Hsf4* gene composed of 13 exons (*dark blue rectangles*). The first three exons and a part of the fourth exon contain sequences that code for the DNA binding domain (DBD, 104 amino acids long). The location of hydrophobic repeats (HR A/B) is indicated. The *open rectangles* indicate alternative exons. The second schematic shows the targeting cassette at the end of the exon 1, an intermediate recombineering step in an unresolved BAC. The targeting cassette contains the LHA and RHA (the *left* and the *right* homologous arms), the EGFP (*green*), two polyadenylation signals (PA, *red*), and neomycin resistance (*neo*, *light blue*) driven by TN5 (*purple*) bracketed by FRT 1 and 2 (*brown*). The *third schematic* shows the BAC after recombination is complete (resolved), which removes the TN5-neo-FRT cassette, leaving the EGFP-Poly A sequences attached to the exon 1 of the *Hsf4* gene and one FRT site in the resolved BAC (*last schematic*). The transgene produces the mRNA for the hybrid gene containing the exon1 sequences of the Hsf4 gene (*dark blue*), the *green* EGFP coding sequences and the polyadenylation sequence (*red*). This mRNA translates into an approximately 32 kDa hybrid protein (N-terminal 41 amino acids [aa] of Hsf4-DBD + 239 aa EGFP).

mice. Anesthesia was avoided because it causes cold cataracts in mice. We found it optimal to examine and record the opacities (Fig. 3) in 21-day-old mice pups, at the age of their weaning. The mouse eyes were dilated with a drop of 1:1 of 0.5% of tropicamide ophthalmic solution and 2.5% of phenylephrine hydrochloride ophthalmic solution (Akorn, Inc., Lake Forest, IL, USA). The images were annotated by Adobe Photoshop Elements 9 (Adobe Systems, San Jose, CA, USA).

Genotyping and Copy Number

Genotyping was performed on DNA extracted from mouse tails[35] using two primer sets; one set within the EGFP cassette to produce a 243-bp amplicon, the other flanking the EGFP to generate a 772-bp amplicon (Fig. 3G). Copy number of the integrated transgene, *Hsf4* (DBD)-EGFP-PolyA-PolyA- FRT BAC was determined as described.[36] The purified Hsf4-EGFP BAC DNA (the end product of our recombineering manipulations, which was used for microinjecting the pronuclei for the generation of the transgenic mice) was used as the standard in the PCR assay ($n = 3$, triplicates/mouse line). The linear equation (Ct versus copy number) was used to estimate the copy number in the unknown sample (transgenic mouse tail DNA). The following copy numbers were determined: N1 = 1, N4 = 1.47, and N7 = 1.62.

Preparation of HSF4-EGFP Reporter Plasmids, Cell Culture, and Transfection

The HSF4b cDNA was obtained by RT-PCR from the RNA of human glioblastoma cell line U373MG[37] by using primer sets (F', 5′-ACTCCACTCCACTCCACACA-3′ and R, 5′-CCAGGAAGC CAAGAAGGAT-3′) according to the manufacturer's protocol (Invitrogen, Carlsbad, CA, USA). It was further amplified by using primer sets (HSF4 F, 5′-AAATTTCTCGA GCGCCACCATG CAGGAAGCGCCAGCTGCGCTG-3′ and HSF4 R, 5′-AAATTT GATA TCTTAGGGGGAGGGACTGGCTTCCGG-3′) and cloned into the pCMV-neo expression vector (Clontech Laboratories, Inc., Mountain View, CA, USA). Next, the EGFP cassette was PCR-amplified from the pBSK plasmid (above) and inserted either into the sequences representing the end of exon1 in the HSF4 cDNA or the end of the exon 13 (c-terminus of HSF4) by using overlapping PCR with the following primers sets: For exon 1 sequences, sense, 5′-CCACCTGATCCGCTG GAGCCCGGTGAGCAAGGGCGAGGAGCTG-3′ and antisense, 5′-CAGCTCCTCGCCCTTGCTCACCGGGCTCCAGCGGATCAG GTGG-3′. For exon 13 sequences, sense, 5′-CCCGGAAGC CAGTCCCTCCCCCGTGAGCAAGGGCGAGGAGCTG-3′ and antisense, 5′-CAGCTCCTCGCCCTTGCTCACGGGGGAGGGAC TGGCTTCCGGG-3′.

A universal primer set starting from the 5′-end of the HSF4 cDNA (forward, 5′-AAATTTCTCGAGCGCCACCATGCAG GAAGCGCCAGCTGCGCTG-3′) and from the C-terminus of EGFP (reverse, 5′-AAATTTGATATCTTACTTGTACAGCT CGTCCATGCC-3′) was used to obtain the final exon1 (DBD)-EGFP and complete HSF4-EGFP cDNA flanked by XhoI and EcoRV sites. The amplified fragments were subcloned into pCMV-neo expression vector.

As a control, an EGFP cDNA also was amplified by PCR (EGFP forward, 5′-AAATTTCTCGAGCGCCACCATGGT GAGCAAGGGCGAGGAGCTG-3′ and EGFP reverse, 5′-AAATTT GATATCTTACTTG TACAGCTCGTCCATGCC-3′) and cloned into the pCMV-neo expression vector. Both of these constructs were transfected permanently into adult human retinal pigment epithelial (ARPE) cells.[37]

Histology, Immunofluorescence, and Immunoblotting

The adult founder and postnatal day two (PND02) lenses were fixed in 4% paraformaldehyde overnight at 4°C before embedding in paraffin. The tissue sections (5 μm) were washed with PBS (×1) and processed either for H&E staining or immunofluorescence as described[19] using anti-αA and anti-αB.[38] Anti- γS raised against mouse γS N-term (EDRNFQGRRYDC; Sigma Genosys, The Woodlands, TX, USA), anti-Fgf7 (Cat. # sc-365440) and anti-Vimentin (Cat. # sc-32322), both monoclonals (Santa Cruz Biotechnology, Inc., Santa Cruz, CA, USA) were

Investigative Ophthalmology & Visual Science

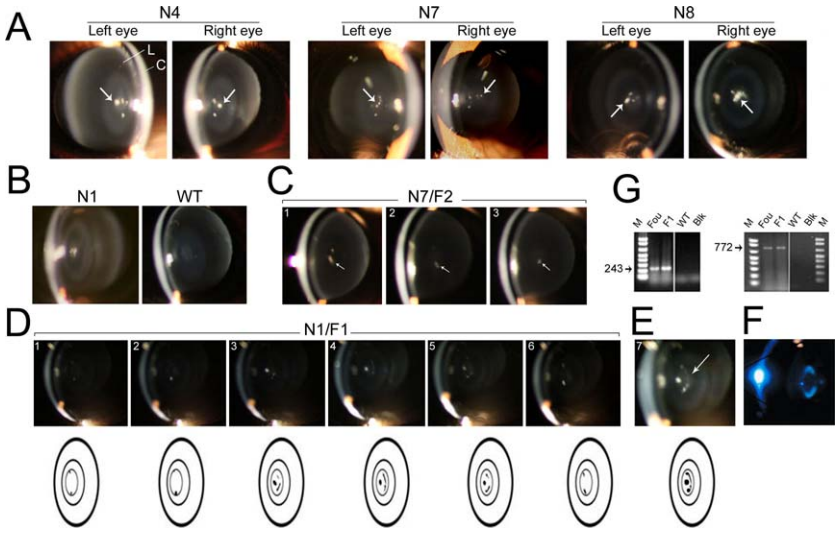

Figure 3. Lamellar opacities appear in the lenses of the transgenic mice generated with *Hsf4 (DBD)-EGFP* transgene. (**A**) Transgenic founders generated with N4, N7, and N8 BACs containing the *Hsf4-EGFP* transgene show bilateral nuclear opacities (*specks*), indicated by *arrows*. Note that the cortex of the lens (L) is clear. C, cornea. (**B**) The N1 transgenic founder mice with discrete lamellar opacities confined to the lens nucleus. WT, age matched wild type. (**C**) Three F2 siblings (21 days old, #1–3) from the N7 founder mice showing dot-like opacities (*arrows*). (**D**) Sequential slit-lamp images (2.5 months old, #1–6) of F1 transgenic mouse lens (from N1 founder, shown in [**B**]). These images were obtained by photographing at different depths. The cataracts appear as *specks* or *dots* of various sizes in the nucleus of the lens (see the corresponding schematics). (**E**) A composite image of all the images shown in (**D**), #1 to 6. The *arrow* points to the arc of opacity. (**F**) Picture of a human lamellar cataract taken from the study of Ionides et al.[44] Reproduced from Ionides A, Francisa P, Berry V, et al. Clinical and genetic heterogeneity in autosomal dominant cataract. *Br J Ophthaolmol*. 1999;83:802–808. Copyright 1999 with permission from BMJ Publishing Group Ltd. (**G**) The presence of the hybrid transgene *Hsf4-EGFP* in founders (Fou) and F1 progeny was confirmed by genotyping using two primer sets, one within the EGFP (amplicon = 243 bp) and other in the flanking exon 1 and EGFP (amplicon = 772 bp). WT, wild type; Blk, no DNA (only N1 data are shown).

used. We used 4′6-diamidino-2-phenylindole (DAPI) to counterstain nuclei. The middle z-section images were acquired using a laser scanning confocal microscope (FluoView FV1000; Olympus Corporation, Tokyo, Japan). All images were analyzed using Image J (available in the public domain at http://imagej.nih.gov/ij), and annotated in Adobe Photoshop Elements version 9.0. In all these studies, we examined multiple lenses (5 lenses/mouse strain).

Total or cytoplasmic and nuclear extracts were made using T-PER or N-PER extraction reagents (Pierce, Rockford, IL, USA) containing protease inhibitor cocktail (Sigma-Aldrich, St. Louis, MO, USA). Immunoblotting was done as described.[19] In the case of the lens, single lenses were used. Anti-Hsf4, rabbit polyclonal antibody raised against the conserved N-terminal sequence (QEAPAALPTEPGPSP; Sigma Genosys) was affinity purified by G protein chromatography before use. This antiserum reacts with the mouse and the human HSF4.[37] Anti-GFP (Catalog #GTX26556; GeneTex, Inc., Irvine, CA, USA) was used to detect the expression of the hybrid protein Hsf4(DBD)-EGFP (~32 KDa). Anti-Gapdh (Catalog #2118S, Cell Signaling Technology, Beverly, MA, USA) also was used with the same immunoblot.[34,37]

2D Gel Electrophoresis and Quantitative RT-PCR (RT-qPCR)

Total protein extracts (40 μg) from PND02 transgenic (N7/F2) and WT lenses were run on IPG strips, pH 3-10 overnight (Bio-Rad Laboratories, Inc., Hercules, CA, USA), followed by gel electrophoresis using 4% to 12% zoom 2D gels (Invitrogen). The gels were stained with Flamingo (Bio-Rad Laboratories, Inc.) and imaged (Fluorchem Q; Alpha Innotech, Santa Clara, CA, USA). The replicate gels were transferred to nitrocellulose membranes for immunoblotting.[19] The 2D-gel analyses were coupled with immunoblotting using specific antibodies for the detection of αB, γS, αA, vimentin, and Fgf7 (in that order). In the immunoblots, therefore, background of the pervious antibody reaction(s) are seen even after "stripping." These can, however, be recognized separate from main reaction(s).

Total RNA was extracted from PND02 lenses of transgenic (N1/F2 and N7/F2) and WT animals, and used for the assay of various transcripts by RT-qPCR[37,39] (primers used are listed in the Table). The RT-qPCR data are presented in two ways: normalized against *Gapdh* as the internal control (mean Ct for *Gapdh* varied by ~0.7–1 cycle between all the samples) and without normalization.

Counting of Epithelial Cells and Fiber Cell Nuclei

Epithelial cells numbers and/or the number of fiber cell nuclei in confocal (DAPI, blue) and H&E images were quantified using Image J software. The pictures were converted to black/white 8 bit images and the background threshold was adjusted. In the next step, the total number of nuclei was obtained by selecting "binary" and "outline" followed by Watershed in the Process tab. Next the images were processed further by selecting "Analyze particles" in the Analysis tab followed by Display results, generating the map of an entire image with number of cells or nuclei. The mean ± SEM is from 3 mice per line (WT and N1/F2 and N7/F2); 6 middle sections were used for these calculations/mouse. The data are presented as bar graphs (Figs. 4, 9).

Statistical Analysis

Student's *t*-tests were performed to compare differences between the groups (WT versus transgenic lens sections). RNA was analyzed from two or three mice per line as indicated in figure legends.

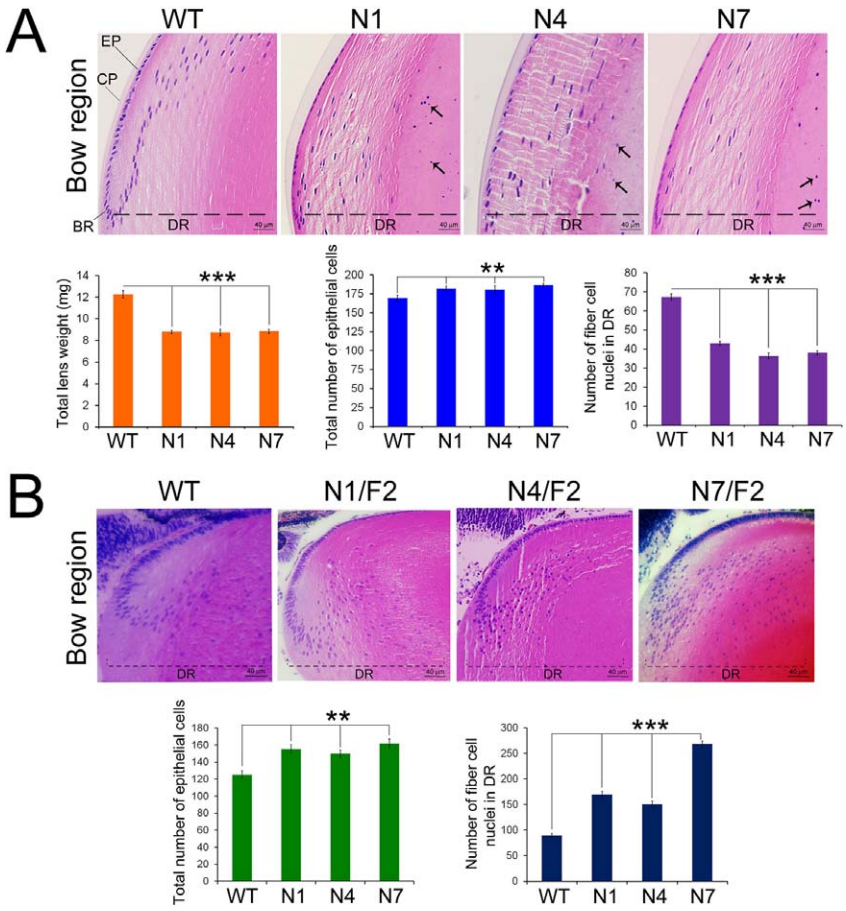

Figure 4. Abnormal secondary fiber cell differentiation in the transgenic lenses. (**A**) Ocular lenses in transgenic founders N1, N4, and N7 show disorganized secondary fiber cell differentiation. The characteristic "bow" region created by the migration of the fiber cell nuclei during differentiation (see WT lens) is not seen in transgenic founders. The shape of the persistent nuclei in transgenic lens also is abnormal (mostly oblong). In the transgenic founders the number of fiber cell nuclei in the differentiation region (marked as DR, *dotted line*) is significantly decreased although the total number of epithelial cells is marginally increased while there is approximately 20% decrease in the lens wet weight (*bar graphs*). (**B**) Equatorial regions PND02 transgenic lenses. Abnormal lens fiber cell nuclei in the lens posterior are evident in N4/F2 and N7/F2 (*arrows*). Vacuoles were observed below lens epithelium and in the superficial cortex of N4 and N7 transgenic mice lines. In N1/F2 transgenic mice, the vacuoles were observed more toward the posterior region of embryonic lens fiber cells (*arrowhead*). The number of fiber cell nuclei in DR and total number of epithelial cells/lens are shown (*bar graphs*).

Results

A key aspect of the hypothesis recounted above is that to achieve the temporal and spatial specificity of interference with *Hsf4* activity, the expression of the transgene must follow the expression of the endogenous gene closely. We used BACs to achieve the temporal and spatial correctness of the expression of the transgene. The BACs, usually 200 to 300 kb long, retain a large portion of the 5′ as well as 3′ sequences and, therefore, the signals surrounding the gene of interest, which are required for the expression that is similar to the endogenous gene activity while avoiding ectopic expression.[40–43] We manipulated four different mouse BACs (N1, N4, N7, N8; Figs. 1, 2) by recombineering[34] (Methods and Fig. 1). An EGFP coding sequence with a polyadenylation signal sequence was inserted at the end of the exon 1 that codes for part of the DBD of the *Hsf4* gene (Figs. 2A, B). Thus, we created a hybrid gene, the *Hsf4* (DBD)-EGFP, to be expressed under the control of a large complement of native DNA sequences surrounding the *Hsf4* gene (Figs. 2A, B, Resolved).

Transgenic Mice Carrying the *Hsf4 (DBD)-EGFP* Hybrid Gene Recapitulate the Human Lamellar Cataract Phenotype

Four transgenic mice lines were produced from four different BACs "recombineered" with the hybrid gene *Hsf4 (DBD)-EGFP* (Figs. 1, 2). The phenotypes of the cataracts obtained with lines N1, N4, N7, and N8 (5 months old) are shown in Figure 3. While the founders show elaborate, but confined nuclear opacities, F2 mice at day 21 show only dots of opacity (Fig. 3C). The composite image (Fig. 3E) and the published image of a human lamellar cataract (Fig. 3F) clearly indicated that we have recreated the lamellar cataract[44] phenotype in the mouse.

Each phenotype shown in Figure 3 can be described as (1) a punctate discrete opacity within the primary nucleus associated with curved opacity, possibly in the same lamellar plane, and/or (2) Multiple discrete opacities, mostly in the primary nucleus, located in different lamellae; in some cases these "dots"/opacities could be connected within an opaque or cataractous fiber. The cataract phenotypes recreated here represent human lamellar opacities described by different names.[44] It must be pointed out that green fluorescent protein

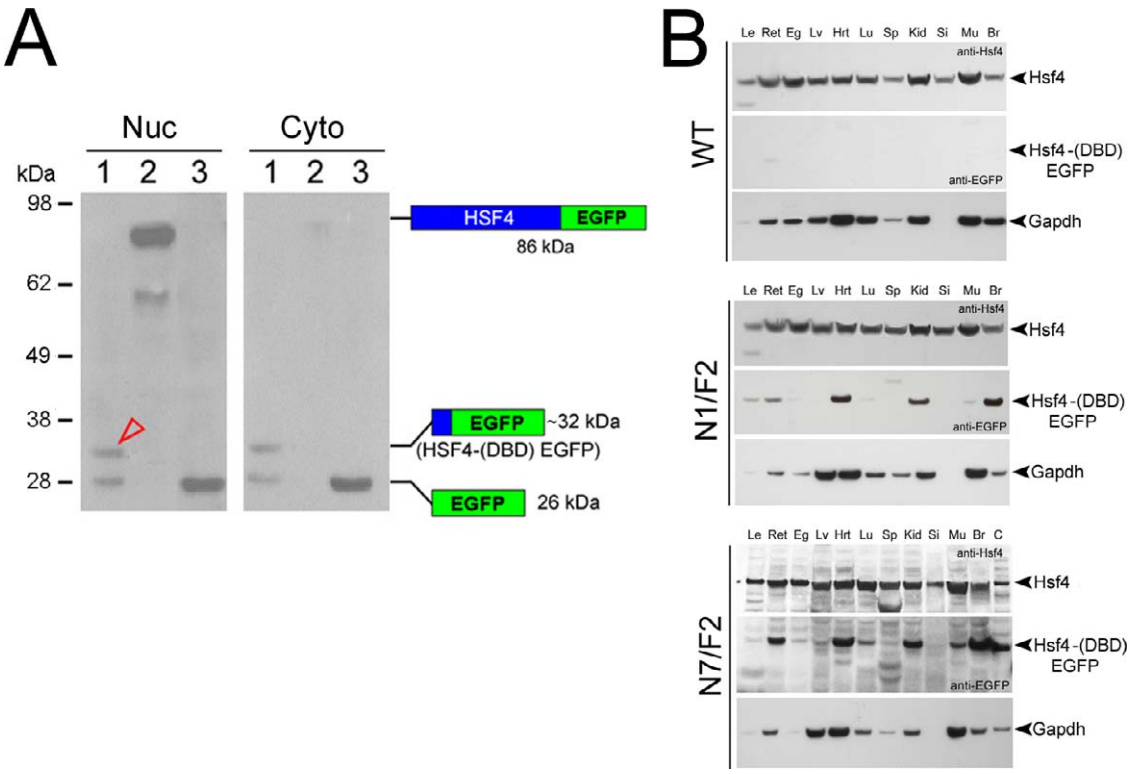

Figure 5. Nuclear location of Hsf4 (DBD)-EGFP in human ARPE cells in culture and expression of the endogenous HSF4 and the transgene in various tissues. (**A**) The ARPE cells were permanently transfected individually with two recombinant constructions: the *Hsf4 (DBD)-EGFP* hybrid and the full length *Hsf4 cDNA-EGFP*. Cell extracts were fractionated and immunoblotted. *Lane 1*: *Hsf4 (DBD)-EGFP* (123 bp of Hsf4 + 720 bp of EGFP produces a ~32 kDa hybrid gene product). *Lane 2*: *Hsf4-EGFP* (approximately 86 kDa hybrid protein). *Lane 3*: native EGFP. Note that Hsf4 (DBD)-EGFP (~32 kDa) is detected in cytoplasmic (Cyto) and nuclear (Nuc) extracts (*open red arrowhead*), while Hsf4-EGFP (86 kDa) is predominantly seen in the nucleus. *Blue*: sequences derived from Hsf4. *Green*: sequences derived from EGFP. (**B**) Expression of the endogenous *Hsf4* and *Hsf4 (DBD)-EGFP* hybrid protein in 11 tissues of PND02 transgenic and WT mouse. EGFP, as expected is not seen in the WT. Each *blot* was made from single tissue samples, thus the lane labeled Le (lens) represents protein sample from one single whole lens. The ratio of the hybrid transgene *Hsf4* as determined by densitometry is 0.73 (N1/F2) and 0.58 (N7/F2) in the lens; however, these values may be underestimations considering that high concentrations of protein (crystallins) in the lens mask low concentration gene products, such as transcription factors. The N7/F2 blot was overexposed for detection in tissues with lower expression. Two different antibodies (anti-Hsf4 and anti-GFP) were used for the upper and the lower halves of the immunoblots, respectively. The last lane in N7/F2, control (C), is a cell extract made from permanently transfected ARPE cells expressing hybrid protein Hsf4 (DBD)-EGFP (~32 kDa). A Gapdh pattern also is presented for each immunoblot as an additional control. Ret, retina; Eg, eye globe; Lv, liver; Hrt, heart; Lu, lung; Sp, spleen; Kid, kidney; Si, small intestine; Mu, muscle; Br, brain.

(GFP) expression within the lens has been used for the study of fiber cell structure and lens morphogenesis,[45] indicating that it does not cause cataracts. Min et al.[30] introduced EGFP after the first codon of *Hsf4* to knock out the *Hsf4* gene; the heterozygous lens, which expresses EGFP presumably has no cataract phenotype.

The Transgenic Lens Shows Defects in Secondary Cell Morphogenesis

Figure 4A shows the status of the equatorial /differentiation zones in the lenses of the founder mice at five months of age. Note that no nuclei are in the center (nucleus) of the lens in the WT; this is because normal differentiation entails degradation of the fiber cell nuclei.[46] This does not happen in the transgenic mice, resulting in the presence of persistent nuclei (Fig. 4, arrows). The lens weights in N1, N4, and N7 founders (5 months of age), show approximately 25% decrease compared to age-matched WT (Fig. 4A, bar graphs). We also see that the number of epithelial cells is increased in these founder lenses, yet the number of total fiber cell nuclei (an indicator of differentiation) is decreased significantly (Fig. 4A, bar graphs), which is consistent with decreased lens weight.

Figure 4B shows lens morphologies in transgenic mice at PND02. Different degrees of disturbances are seen in the bow region in all of them with nuclei seen even in the posterior of the lens. Interestingly, the number of total epithelial cells shows an increase in these lenses as observed in the founder mice (Fig. 4A). However, unlike the founders (which are older mice) the number of fiber cell nuclei in the PND02 lens shows an increase in the differentiation region (DR; Fig. 4B, bar graphs). The largest increase is seen in the N7/F2 mice, which show the most abnormality.

The *Hsf4 (DBD)-EGFP* Hybrid Gene Product Translocates to the Cell Nucleus

We engineered the *Hsf4 (DBD)-EGFP* hybrid under the control of the CMV promoter and made permanently transfected human ARPE19 cells to assess the intracellular distribution of the hybrid protein. The hybrid gene product, a 32 kDa protein (41 residues of *Hsf4* and 239 residues of the EGFP), is detected in the cytoplasm as well as in the nucleus of these cells (Fig. 5A, lane 1). We also expressed a complete *Hsf4*-EGFP hybrid (86 kDa protein) in these cells and it is found predominantly in the nucleus (Fig. 5A, lane 2). The presence of the hybrid gene product in the nucleus is corroborated by the staining of the

Investigative Ophthalmology & Visual Science

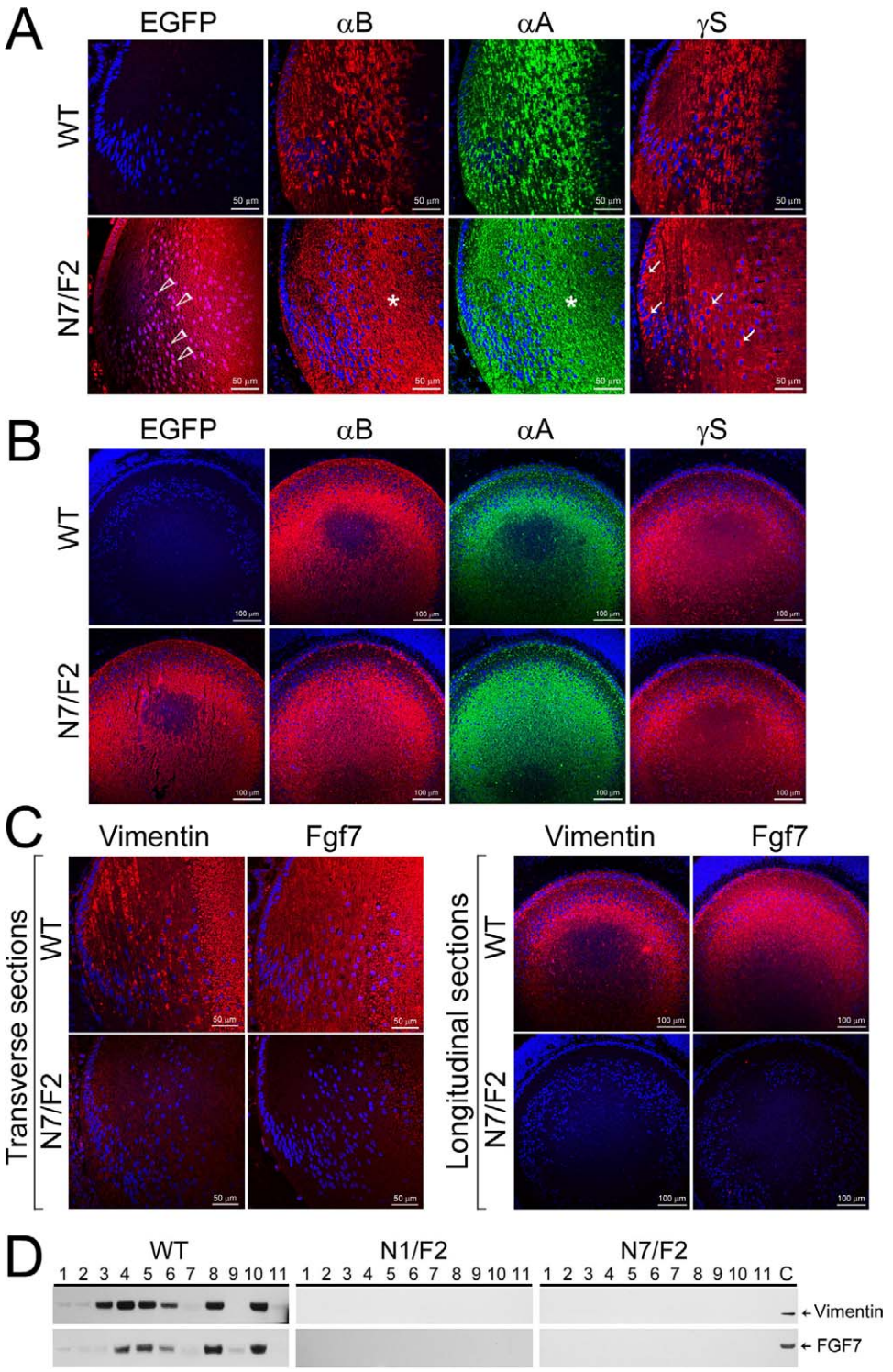

Figure 6. Altered distribution patterns of αA, αB, and γS, and loss of Vimentin and Fgf 7 expression in PND02 transgenic mouse lens. (**A**) Immunofluorescence and laser scanning confocal images (transverse/anteroposterior axis) show expression of EGFP (*red*) in N7/F2 (*open arrowheads*) and its absence in the WT. The staining patterns of αA (*green*) and αB (*red*) show homogenous or granular distribution (*asterisks*), while γS shows pools of staining (*red*, possibly aggregated protein, *arrows*) around the nuclei (*blue*). Compare this staining pattern with the staining in the first (EGFP) column (N7/F2). The nuclei in the EGFP column are *violet* (a mix of *blue* and *red*, *open arrowheads*) , we do not see violet nuclei in the γS-stained section, that is because γS is a cytoplasmic protein, while Hsf4(DBD)-EGFP hybrid is a nuclear as well as a cytoplasmic protein. (**B**) Longitudinal views (perpendicular to anteroposterior axis) of αA, αB, and γS staining in the PND02 lens confirm what is seen in (A). (**C**) Transverse sections (*left*) and longitudinal views (perpendicular to anteroposterior axis (*right*) show loss of vimentin and Fgf7 expression in PND02 transgenic lens. The anteroposterior streaks of vimentin are seen in the WT lens. The staining pattern of Fgf7 is more homogenous all through the cortex in WT lens. (**D**) Immunoblots showing vimentin and Fgf7 presence in various tissues in the WT mice (*1*, lens; *2*, retina; *3*, eye globe; *4*, liver; *5*, heart; *6*, lung; *7*, spleen; *8*, kidney; *9*, small intestine; *10*, muscle; and *11*, brain; C, control lens extract). However, these proteins are not detected in any of the tissues examined in PND02, N1/F2 and N7/F2 animals.

Investigative Ophthalmology & Visual Science

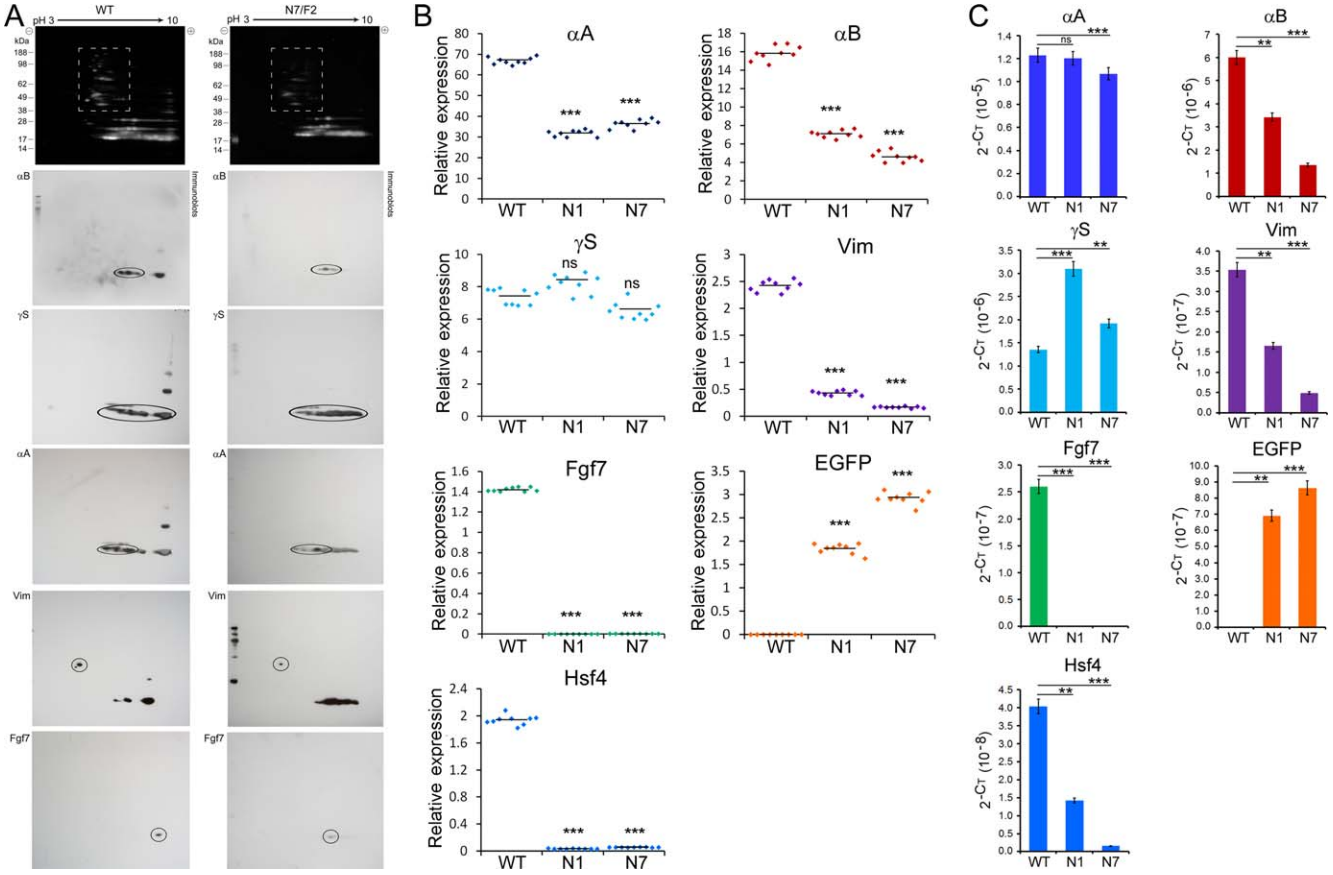

Figure 7. Expression of crystallins, vimentin, and Fgf7 in PND02 transgenic lens. (**A**) The *top* shows Flamingo-stained fluorescent gels with standards (KDa). Note loss of higher molecular weight proteins (*dotted box*) in N7/F2. In the *lower parts* antibody reactions have been *circled*. One immunoblot was used with repeated stripping. The background reactions, when seen, are mostly *gray/black* reactivities. Anti-γS cross reacts with γ-crystallins in the WT as well as in N7/F2 blots. Note appreciable decreases in αB and αA, and also in vimentin (Vim) and Fgf7. (**B**) RT–qPCR analysis of WT, N1/F2, and N7/F2 PND02 RNA presented as relative gene expression using *Gapdh* as the internal control. Raw data points (normalized, $2^{-\Delta\Delta CT}$) are shown in *dot plots*. The means are indicated by a *horizontal black line* across the points. These data corroborate what is seen in the 2D-gels. (**C**) RT-qPCR data, presented in (**B**) were analyzed without normalization and presented in *bar graphs* (a 2^{-CT} plot[60]). Note these data show changes in the transcript levels of γS. The hybrid *Hsf4 (DBD)-EGFP* transcripts were detected using EGFP-specific primers. The data represent three experimental replicates from three independent biological samples. $^{***}P < 0.001$ and $^{*}P < 0.01$ were considered to be statistically significant. ns, not significant.

fiber cell nuclei by anti-EGFP (see Fig. 6A, compare N7/F2, first picture with three other pictures). These data confirm previously reported translocation of EGFP and EGFP-hybrid proteins to the cell nucleus.[47–49] Note that in the cytoplasmic as well as in the nuclear extracts (lane 1) we see a band around 26 KDa reacting to anti-GFP, suggesting cleavage of the hybrid gene product. On the other hand we do not see these bands in the total extracts of 11 transgenic tissues (Fig. 5B).

The endogenous *Hsf4* and the transgene encoded *Hsf4 (DBD)-EGFP* hybrid proteins are detected in multiple tissues, including the ocular lens in the PND02 transgenic mice (Fig. 5B). A corresponding Gapdh pattern also is shown in each of the immunblots. While varying levels of the hybrid transgene (*Hsf4 [DBD]-EGFP*) protein are detected, there are comparable levels of endogenous Hsf4 in WT, N1/F2, and N7/F2 transgenic tissues.

Status of Various Gene Products in the Transgenic Lens

We examined the expression of αA-crystallin (αA), αB-crystallin (αB), γS-crystallin (γS), vimentin, and fibroblast growth factor 7 (Fgf7) in the PND02 transgenic mouse lens. Note that αA, αB are few of the very early gene products that are synthesized during the ocular lens development.[50] αA is one of the main structural proteins in the lens.[51,52] γS is one of the main postnatal lens crystallins,[53] while vimentin is a cytoskeletal protein, important for lens architecture; Fgf7 has been reported to be the chief growth factor whose expression is increased in 6-week-old *Hsf4* knockout (KO) mice.[29] The expression of these gene products was assessed by confocal immunohistochemistry (Figs. 6A–C), immunoblotting (Fig. 6D), 2D gel electrophoresis/immunoblotting (Fig. 7A), and RT-qPCR (Figs. 7B, 7C).

Although confocal immunofluorescence did not suggest a large alteration in the expression of αA, αB, and γS, it revealed their abnormal distribution in the differentiating fiber cells (Figs. 6A, 6B). Both αA and αB, showed an amorphous distribution in the transgenic lenses (Fig. 6A, N7/F2; αA, αB, asterisks) as opposed to streaks of protein that run along the anteroposterior axis of the fiber cell in the WT.[19,38] The γS staining was obvious because of its abnormal distribution, showing pools of potentially aggregated protein around the nuclei in transgenic lenses (Fig. 6A, N7/F2, γS, arrows). Vimentin and Fgf7 are hardly detectable by confocal immunohistochemistry in the transgenic lens, N7/F2 (Fig. 6C); their undetectable expression is confirmed in single lens immunoblots of the PND02 lens protein (Fig. 6D).

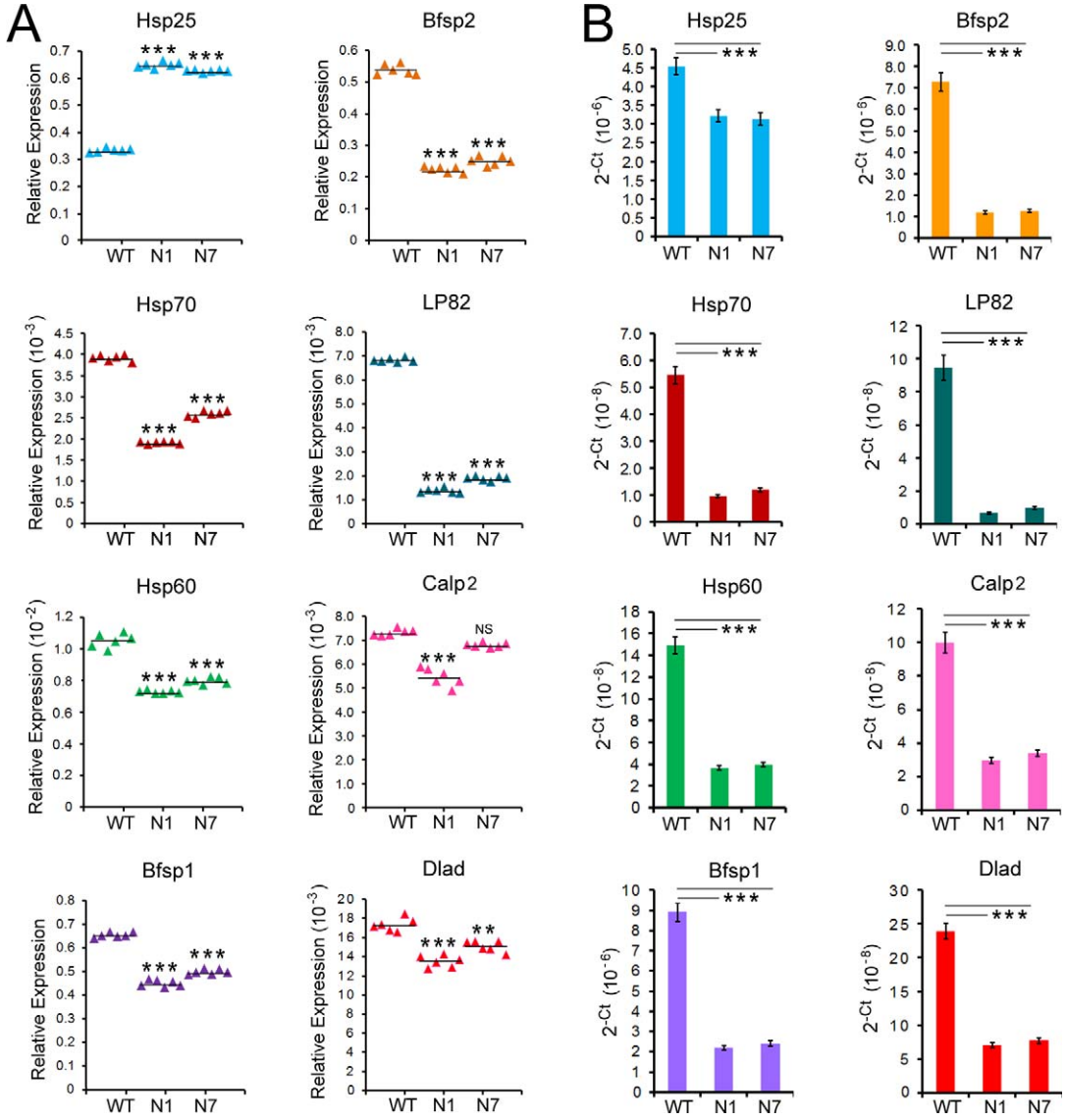

Figure 8. Transcripts levels of *Hsf4*-associated target genes in the PND02 in WT and transgenic lenses (N1 and N7). The transcript were chosen on the basis of their association with Hsf4, being directly or indirectly impacted by *Hsf4* KO.[29–31] The data are plotted with normalization based on *Gapdh* as the internal control (**A**) and without normalization (**B**) as in Figure 7. The *Hsp70* and *Hsp60* transcripts decreased by 1.5- to 6-fold in N1/F2 and N7/F2 transgenic RNA. The transcripts of *Bfsp1* and *2* show 2- to 6-fold decrease in either calculation (normalized or without normalization). The *Dlad*, a DNase 2, which may be involved in the degradation of the nuclei,[61,62] shows approximately a 2-fold decrease in its transcript level, when the data were normalized, but approximately a 5-fold decrease in data without normalization. *Lp82* (calpain3) and *calpain 2* also show similar decreases. Note that *Hsp25* shows approximately a ×2 increase in expression when using normalization (**A**) and approximately a ×1.5 decrease without normalization (**B**). $^{***}P < 0.001$ and $^{**}P < 0.01$ were considered to be statistically significant.

The 2D gel electrophoresis and immunoblotting data show appreciable decreases in αA and αB (Fig. 7A). Although these immunoblots are not quantitative, vimentin and Fgf7 show noteworthy reductions in their respective contents (Figs. 6D, 7A). All of these observations are confirmed by RT-qPCR of the respective transcript levels (Figs. 7B, 7C) validating what is seen in 2D gel immunoblots. Note that the γS transcript levels did not show significant change (when data are plotted with normalization against *Gapdh*, Fig. 7B); however, the same data when plotted without normalization in Figure 7C show an increase. We choose to present the RT-qPCR data in two different ways, because housekeeping genes (e.g., *Gapdh*) are not always present at constant levels (for example, see Fig. 5B immunoblot) and, therefore, cannot be used confidently on the basis that they do not change. The data without normalization give an assessment of what it would look like on a per lens basis (total RNA) assuming that everything else remained constant.

Interestingly the transcript levels of the endogenous *Hsf4* are remarkably reduced in transgenic lenses (Figs. 7B, 7C), but we do not see corresponding decrease in Hsf4 protein levels in the lens (Fig. 5B, lane 1). There seem to be comparable levels of Hsf4 protein in the WT and in the transgenic animals in all tissues (Fig. 5B).

The *Hsf4* KO studies[29–31] have suggested many targets for this transcription factor. Therefore, we investigated eight additional gene transcript levels by RT-qPCR (Fig. 8). These data again were analyzed in two different ways as was done in Figures 7B and 7C. All transcripts (*Hsp70*, *Hsp60*, *Bfsp* [beaded filament structural protein] 1 and 2, *Lp82* [Calpain 3], *Calp2* [Calpain 2], and *DLAD* [DNase II-like acid DNase/DNase IIβ])

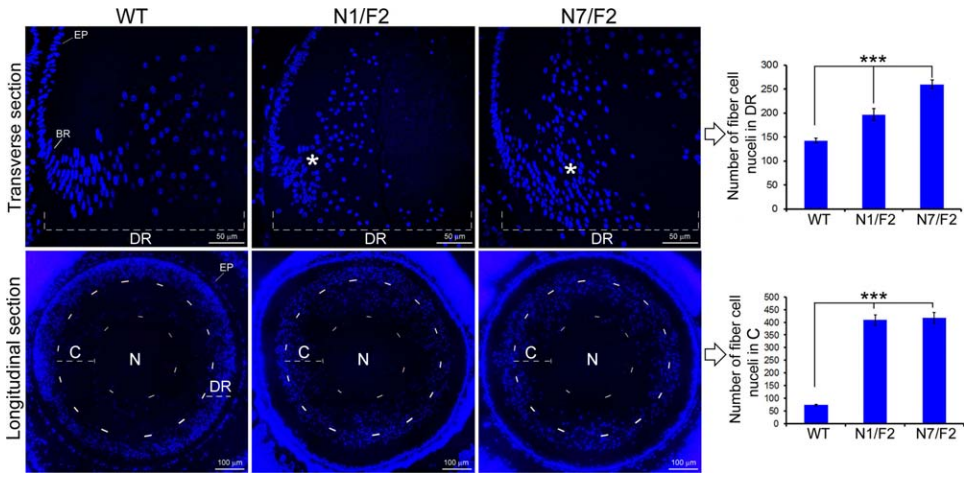

Figure 9. Accumulation of differentiating fiber cell nuclei in the PND02 transgenic lenses. In the *top*, transverse (anteroposterior axis) sections from WT, and N1/F2 and N7/F2 lenses stained with DAPI are shown. Note the presence of elongated nuclei in the bow region of the WT. A close examination reveals that there are no elongated nuclei in the differentiating region of the transgenic lenses. There is, however, a preponderance of doughnut-shaped nuclei in N1/F2 and N7/F2 lenses (*asterisks*). The number of the nuclei in the DR was calculated and is presented as a *bar graph* on the *right side*. In the *bottom*, longitudinal (perpendicular to anteroposterior axis) sections reveal an abnormal distribution of the fiber cell nuclei in transgenic lenses (N1/F2 and N7/F2). In the WT lens, very few degenerating nuclei are seen in the center or the nucleus (N) of the lens, which has been demarcated with an *arbitrary circle*. We placed an *additional circle* equidistant from the *inner circle* in the cortex of the lenses in the WT and transgenic lenses, and counted the number of nuclei in this space (C). These data are presented as a *bar graph* on the *right side*. Note also that in the *upper part* the magnification bar is 50 μm and in the *lower part* it is 100 μm. These images were acquired using FSX-100 Olympus microscope. EP, epithelium; BR, bow DR.

showed decreased levels, except in the case of Hsp 25, which upon normalization with *Gapdh* showed a ×2 increase.

Abnormal Distribution of Differentiating Nuclei in the Transgenic Lens

The data presented in Figures 4 and 6 suggest that the differentiation of the lens fiber cells in the transgenic mice is not normal. A quantitative assessment of the distribution of the fiber cell nuclei reveals an increase in the number of fiber cell nuclei in the DR, in the PND02 transgenic lens (Figs. 4B, 9, bar graphs). On the other hand, the transgenic founder lenses show a decrease in the number of fiber cell nuclei (Fig. 4A, bar graphs). Importantly, this observation is corroborated by the data obtained from the transverse as well as longitudinal sections of the lens. These data suggest a potential association between the transparent adult lens cortex and decreased fiber cell nuclei retention. Conversely, increased number of fiber cell nuclei in PND02 transgenic lens may suggest an association with the lamellar cataract phenotype, although this speculation must be confirmed with additional cell proliferation studies.

Discussion

The data presented here demonstrate recapitulation of developmentally dictated and morphologically confined nuclear opacities produced in the transgenic mouse lens as a result of biologically relevant expression of *Hsf4 (DBD)-EGFP* transgene. These cataracts are similar to the human lamellar cataract.[44] The pathology is not rampant; the cataract does not take over every fiber cell of the lens. It is notable, therefore, that *Hsf4* null (absence of the gene product) studies report total lens cataracts[29,31] attended by anterior segment pathologies and severe changes in lens morphology, including the capsule rupture.[29,54] It is possible that we may find molecular similarities with *Hsf4* KO lenses, because the lamellar phenotype may be camouflaged within the total cataracts in these lenses.

The generation of similar disease phenotypes using four different BACs in four different lines of transgenic mice indicates that the disruption of the DBD can be achieved functionally by the insertion of an EGFP sequence (Fig. 1) to generate a dominant phenotype similar to a mutation in the DBD of the *Hsf4* gene. The morphologic appearance of the phenotype (Fig. 3) suggests specific activity involving the hybrid gene product, which contains the whole N-terminus of the Hsf4 polypeptide (41 residues in all including 23 amino acids of the DBD) attached to the N-terminus of EGFP. The truncation of the Hsf4 protein, away from the C-terminal part of the Hsf4 protein may have contributed to the generation of a highly specific interference with the DBD function to produce the confined cataract phenotype in the transgenic mice. Although there may be variations in the phenotype related to the expression of the hybrid transgene because of the different lengths of the 5′ upstream sequences (Fig. 2A, 50–202 kb), one phenotype that remains consistent is the disturbance in the secondary fiber cell differentiation and the persistence of fiber cell nuclei. This is in agreement with BAC-driven expression of heterologous reporter genes in specific neuroanatomical locations in the brain and other tissues.[55,56] It also is important to consider that the dominant negative gene products may not cause complete inhibition of the native activity as seen in KOs. The appearance of a phenotype will depend on the timing of expression, and the effective concentrations of the endogenous and dominant negative gene products.

The fact that the expression of the transgene *Hsf4 (DBD)-EGFP* leads to Lamellar cataracts in the mouse lens, similar to the phenotypes seen in the human lens, suggests involvement of conserved physiologic functions related to the DNA binding domain of the *Hsf4* gene in the lens development. Additionally, these data provide direct experimental support for the assertion that the human and mouse lens growth is controlled by similar principles, independent of their respective life spans.[57]

Hsf4 null/KO studies have suggested that deletion of the *Hsf4* gene alters the expression of many genes in the

Investigative Ophthalmology & Visual Science

Table. Total RNA Was Extracted From Mouse Tissues by TRIzol Plus RNA Purification System (Invitrogen)

1	*CryαA*:	F: 5′-gagattcacggcaaacacaa-3′
		R: 5′-aaattcacgggaaatgtagcc-3′
2	*CryαB*:	F: 5′-cctgagcccttctaccttc-3′
		R: 5′-tccttctccaaacgcatctc-3′
3	*Cryγs*:	F: 5′-gaataccagcgttggatgg-3′
		R: 5′-gaaggacagtcttccgtgg-3′
4	*Vim*:	F: 5′-ccaacctttttcttccctgaa-3′
		R: 5′-tgagtgggtgtcaaccagag-3′
5	*Fgf7*:	F: 5′-cagacagcagacacggaac-3′
		R: 5′-gcctcctcctatttgtgaac-3′
6	*EGFP*:	F: 5′-cttcttcaagtccgccat-3′
		R: 5′-caccttgatgccgttcttct-3′
7	*Hsf4*:	F: 5′-gagccacagtcagcagcac-3′
		R: 5′-cgctcccctcatctagca-3′
8	*Gapdh*:	F: 5′-ggtgaaggtcggtgttgaacg-3′
		R: 5′-ctcgctcctggaagatggtg-3′
9	*Hsp25*:	F: 5′-ggaagtctgaacagtctgga-3′
		R: 5′-gtatcaaaagagcgcacag-3′
10	*Hsp70*:	F: 5′-cagtagcctgggaagacata-3′
		R: 5′-tagtacacagtgccaagacg-3′
11	*Hsp60*:	F: 5′-cagagttcctcagaagttgg-3′
		R: 5′-catccagtaaggcagttctc-3′
12	Bfsp1:	F: 5′-acagacaagaatgggttacg-3′
		R: 5′-aggtatgatcacaggacagg-3′
13	*Bfsp2*:	F: 5′-ggctttctgtcaagaagcta-3′
		R: 5′-ctcaaggacatcatccagac-3′
14	*LP82*:	F: 5′-acacagaccaggaaagtgag-3′
		R: 5′-tgtgttgaggacattcttga-3′
15	*Calp2*:	F: 5′-attctggatgtccttcagtg-3′
		R: 5′-ttggtgagtttccacttctt-3′
16	*Dlad*:	F: 5′-gacagcaaagcctctaagaa-3′
		R: 5′-gtccacagcttcaccatatt-3′

Approximately 1 μg of total RNA was treated by DNase I (Invitrogen) and reverse transcribed by using Superscript III (Invitrogen) in 20 μl. For RT-qPCR, 1 μL of cDNA was amplified with a SYBR Green Master mix for 45 cycles (Hoffmann-La Roche, Basel, Switzerland) and analyzed as described.[37] Primers used for RT-qPCR (Figs. 7B, 7C, 8A, 8B) are shown above. F, forward; R, reverse.

lens.[29–31,58] Although there is no consensus about the status (absence or presence) of various gene products in the *Hsf4* KO studies,[29–31] we have used these studies as a basis for assessing the status of αA, αB, γS, vimentin, and Fgf7 in our model. This was done by immunocytochemistry (Fig. 6), 2D-immunoblotting (Fig. 7A), and by the assessment of the corresponding transcript levels (Figs. 7B, 7C). Immunostaining reveals abnormal distribution patterns of crystallins (αA, αB) in the transgenic lens (Fig. 6). The data presented in Figure 7 show that there is a general decrease in crystallin gene expression. While the data obtained with γS transcript levels are subject to different interpretations based on how it is plotted (Figs. 7B, 7C), confocal immunostaining reveals abnormal γS distribution as pools of aggregated protein surrounding the fiber cell nuclei (Fig. 6A).

Interestingly, we also see a large decrease in *Hsf4* transcripts, but this is not mirrored in the level of the Hsf4 protein (Fig. 5B), suggesting that the presence of the hybrid gene transcript/protein may interfere with the stability of the endogenous *Hsf4* transcripts in addition to working as a dominant negative.

Importantly, a decrease in vimentin expression and an almost total absence of Fgf7 is observed (Figs. 6C, 6D) at the protein (Fig. 7A) as well as at the RNA transcript (Figs. 7B, 7C) levels. This is in contrast to reported increase in *Fgf7* transcript levels in 6-week-old *Hsf4* KO lenses[29]; however, in these studies it was not clear if there was a corresponding increase in the Fgf7 protein. A direct comparison, nonetheless, on the basis of our determinations, between the KO work and our work may be unwarranted, considering that in the KO studies the phenotype (a severe cataract) is different from the phenotype generated in our work, which is a discreet opacity (a dot or streak) involving only a few fiber cells (Fig. 3). This is borne out by general downregulation of eight additional transcripts in these transgenic mice (Fig. 8). It is obvious that, while the KO work highlights the importance of *Hsf4* for critical regulatory function in the postembryonic/postnatal lens, it may be of limited use in assessing the lamellar cataract phenotype mechanistically.

The data presented in Figures 4 and 9 clearly establish that, in comparison to the WT, the degeneration and persistence of fiber cell nuclei is a hallmark of the lamellar cataract phenotype. In light of these data, the decrease in fiber cell nuclei in the adult founder lenses (Fig. 4A) in comparison with the increase in fiber cell nuclei in the young PND02 transgenic lens (Fig. 4B) is highly informative. Considering that the growth of the adult lens is comparatively slower than in the early postnatal lens,[57] it is tempting to surmise that slow growth/differentiation (lesser number of fiber cell nuclei), may be the basis of the clear cortex in the adult lens (Fig. 4A). Conversely, high growth rate (large number of persistent nuclei), in the PND02 transgenic lens (Figs. 4B, 9), may contribute to lamellar cataract pathogenesis. Interestingly, the confocal images shown in Figure 9 for the transgenic lenses look similar to the description of this pathology in the human lens by Marner et al.[10] in 1989. The relationship between these observations and lamellar cataract phenotype must await further investigations on the molecular progression of the fiber cell nuclei degeneration[46] in this transgenic paradigm.

Finally, we recognize the limitations in this study. We believe that the molecular pathogenesis, which cannot be observed with the slit-lamp, precedes the morphologic pathology. The opacities were observed by slit-lamp at 21 days (F2s, see Fig. 3) while the molecular changes, for example seen in Figure 6 (distribution of crystallins), are seen at PND02, wherein the data seem to suggest global changes in the lens fiber cells, yet the pathology matures to a cataractous, morphologically recognizable phenotype only in specific lamellae. These molecular changes observed at this time cannot be causally related to the cataractous changes in specific fiber cells; it is clear that the reduction of vimentin and/or Fgf7 expression is not casually linked to the lamellar cataract. It also is clear that the expression of the hybrid transgene does not relate to specific fiber cell cataractogenesis. We hypothesize that the progression of molecular pathogenesis initiated by the hybrid transgene is fiber cell–specific in the backdrop of the gene activity dictated by *Hsf4*, suggesting heterogeneity in the gene expression controlled by this transcription factor in different fiber cells.

While it is obvious from the morphological diversity of the human cataracts[44] that the ocular lens fiber cells are physiologically heterogeneous; the recreation of the lamellar cataract further establishes the heterogeneity of the fiber cell gene expression as modulated by *Hsf4*. A molecular description of this heterogeneity is essential to an understanding of the mechanism that leads to the pathogenesis of the human lamellar cataract.

Acknowledgments

The authors thank Bridgette Gomperts and Derrick Nickerson for their advice and the gift of the pBSK plasmid containing the Tn5-Neo cassette; Joseph Horwitz, Kevin Miller, and Sherwin Isenberg

Investigative Ophthalmology & Visual Science

for their advice and input; Ishanee Dighe for technical assistance; Alberto Valencia for his help in procuring the ophthalmoscope; Joanne L Zahorsky-Reeves and Sonia Watt (Division of Laboratory Animal Medicine, UCLA personnel) for help with the maintenance and breeding of the transgenic animals; and Joanna Gallino and Anastasia Schimmel for helping with the cryopreservation of the transgenic embryos.

Supported by a National Institutes of Health (Bethesda, MD, USA) grant (SPB) and Gerald Oppenheimer Family Foundation Center for the Prevention of Eye Disease Program.

Disclosure: **R.K. Gangalum**, None; **Z. Jing**, None; **A.M. Bhat**, None; **J. Lee**, None; **Y. Nagaoka**, None; **S.X. Deng**, None; **M. Jiang**, None; **S.P. Bhat**, None

References

1. Zetterstrom C Kugelberg M. Paediatric cataract surgery. *Acta Ophthalmol Scand*. 2007;85:698–710.
2. Chen TC, Bhatia LS, Halpern EF, Walton DS. Risk factors for the development of aphakic glaucoma after congenital cataract surgery. *Trans Am Ophthalmol Soc*. 2006;104:241–251.
3. Haargaard B, Ritz C, Oudin A, et al. Risk of glaucoma after pediatric cataract surgery. *Invest Ophthalmol Vis Sci*. 2008;49: 1791–1796.
4. Lambert SR, Purohit A, Superak HM, Lynn MJ, Beck AD. Long-term risk of glaucoma after congenital cataract surgery. *Am J Ophthalmol*. 2013;156:355–361.
5. Francis PJ Moore AT. Genetics of childhood cataract. *Curr Opin Ophthalmol*. 2004;15:10–15.
6. Hejtmancik JF. Congenital cataracts and their molecular genetics. *Semin Cell Dev Biol*. 2008;19:134–149.
7. Falls HF. Developmental cataracts: results of surgical treatment in one hundred and thirty-one cases. *Arch. Ophthalmol*. 1943; 29:210–223.
8. Forster JE, Abadi RV, Muldoon M, Lloyd IC. Grading infantile cataracts. *Ophthalmic Physiol Opt*. 2006;26:372–379.
9. Francis PJ, Berry V, Bhattacharya SS, Moore AT. The genetics of childhood cataract. *J Med Genet*. 2000;37:481–488.
10. Marner E, Rosenberg T, Eiberg H. Autosomal dominant congenital cataract. Morphology and genetic mapping. *Acta Ophthalmol (Copenh)*. 1989;67:151–158.
11. Bhat SP. The ocular lens epithelium. *Biosci Rep*. 2001;21:537–563.
12. Graw J. Mouse models of cataract. *J Genet*. 2009;88:469–486.
13. Bloemendal H, Raats JM, Pieper FR, Benedetti EL, Dunia I. Transgenic mice carrying chimeric or mutated type III intermediate filament (IF) genes. *Cell Mol Life Sci*. 1997;53: 1–12.
14. Srinivasan Y, Lovicu FJ, Overbeek PA. Lens-specific expression of transforming growth factor beta1 in transgenic mice causes anterior subcapsular cataracts. *J Clin Invest*. 1998;101:625–634.
15. Tumminia SJ, Clark JI, Richiert DM, et al. Three distinct stages of lens opacification in transgenic mice expressing the HIV-1 protease. *Exp Eye Res*. 2001;72:115–121.
16. Varadaraj K, Kumari SS, Mathias RT. Transgenic expression of AQP1 in the fiber cells of AQP0 knockout mouse: effects on lens transparency. *Exp Eye Res*. 2010;91:393–404.
17. Andley UP, Reilly MA. In vivo lens deficiency of the R49C alphaA-crystallin mutant. *Exp Eye Res*. 2010;90:699–702.
18. Bhat SP. Transparency and non-refractive functions of crystallins–a proposal. *Exp Eye Res*. 2004;79:809–816.
19. Gangalum RK, Bhat SP. AlphaB-crystallin: a Golgi-associated membrane protein in the developing ocular lens. *Invest Ophthalmol Vis Sci*. 2009;50:3283–3290.
20. Puk O, Ahmad N, Wagner S, Hrabe de Angelis M, Graw J. First mutation in the betaA2-crystallin encoding gene is associated with small lenses and age-related cataracts. *Invest Ophthalmol Vis Sci*. 2011;52:2571–2576.
21. Rao NA, Saraswathy S, Wu GS, et al. Elevated retina-specific expression of the small heat shock protein, alphaA-crystallin, is associated with photoreceptor protection in experimental uveitis. *Invest Ophthalmol Vis Sci*. 2008;49:1161–1171.
22. Shi Y, Shi X, Jin Y, et al. Mutation screening of HSF4 in 150 age-related cataract patients. *Mol Vis*. 2008;14:1850–1855.
23. Shiels A, Hejtmancik JF. Genetics of human cataract. *Clin Genet*. 2013;84:120–127.
24. Smaoui N, Beltaief O, BenHamed S, et al. A homozygous splice mutation in the HSF4 gene is associated with an autosomal recessive congenital cataract. *Invest Ophthalmol Vis Sci*. 2004;45:2716–2721.
25. Liang L, Liegel R, Endres B, , et al. Functional analysis of the Hsf4(lop11) allele responsible for cataracts in lop11 mice. *Mol Vis*. 2011;17:3062–3071.
26. Bu L, Jin Y, Shi Y, et al. Mutant DNA-binding domain of HSF4 is associated with autosomal dominant lamellar and Marner cataract. *Nat Genet*. 2002;31:276–278.
27. Enoki Y, Mukoda Y, Furutani C, Sakurai H. DNA-binding and transcriptional activities of human HSF4 containing mutations that associate with congenital and age-related cataracts. *Biochim Biophys Acta*. 2010;1802:749–753.
28. Akerfelt M, Trouillet D, Mezger V, Sistonen L. Heat shock factors at a crossroad between stress and development. *Ann N Y Acad Sci*. 2007;1113:15–27.
29. Fujimoto M, Izu H, Seki K, et al. HSF4 is required for normal cell growth and differentiation during mouse lens development. *Embo J*. 2004;23:4297–306.
30. Min JN, Zhang Y, Moskophidis D, Mivechi NF. Unique contribution of heat shock transcription factor 4 in ocular lens development and fiber cell differentiation. *Genesis*. 2004; 40:205–217.
31. Shi X, Cui B, Wang Z, et al. Removal of Hsf4 leads to cataract development in mice through down-regulation of gamma S-crystallin and Bfsp expression. *BMC Mol Biol*. 2009;10: 10.
32. Somasundaram T, Bhat SP. Developmentally dictated expression of heat shock factors: exclusive expression of HSF4 in the postnatal lens and its specific interaction with alphaB-crystallin heat shock promoter. *J Biol Chem*. 2004;279: 44497–44503.
33. Nakai A, Tanabe M, Kawazoe Y, et al. HSF4, a new member of the human heat shock factor family which lacks properties of a transcriptional activator. *Mol Cell Biol*. 1997;17:469–481.
34. Gangalum RK, Jing Z, Nagaoka Y, Jiang M, Bhat SP. Purification of BAC DNA for high-efficiency transgenesis. *Biotechniques*. 2011;51:335–336.
35. Miralves J, Magdeleine E, Joly E. Design of an improved set of oligonucleotide primers for genotyping MeCP2tm1.1Bird KO mice by PCR. *Mol Neurodegener*. 2007;2:16.
36. Joshi M, Keith Pittman H, Haisch C, Verbanac K. Real-time PCR to determine transgene copy number and to quantitate the biolocalization of adoptively transferred cells from EGFP-transgenic mice. *Biotechniques*. 2008;45:247–258.
37. Jing Z, Gangalum RK, Lee JZ, Mock D, Bhat SP. Cell-type-dependent access of HSF1 and HSF4 to alphaB-crystallin promoter during heat shock. *Cell Stress Chaperones*. 2013;18: 377–387.
38. Gangalum RK, Horwitz J, Kohan SA, Bhat SP. AlphaA-crystallin and alphaB-crystallin reside in separate subcellular compartments in the developing ocular lens. *J Biol Chem*. 2012;287: 42407–42416.

Investigative Ophthalmology & Visual Science

39. Livak KJ, Schmittgen TD. Analysis of relative gene expression data using real-time quantitative PCR and the 2(-delta delta c(t)) method. *Methods*. 2001;25:402–408.
40. Heintz N. BAC to the future: the use of bac transgenic mice for neuroscience research. *Nat Rev Neurosci*. 2001;2:861–870.
41. Hofemeister H, Ciotta G, Fu J, et al. Recombineering, transfection, Western, IP and ChIP methods for protein tagging via gene targeting or BAC transgenesis. *Methods*. 2011;53:437–452.
42. Huang Y, Liu DP, Wu L, et al. Proper developmental control of human globin genes reproduced by transgenic mice containing a 160-kb BAC carrying the human beta-globin locus. *Blood Cells Mol Dis*. 2000;26:598–610.
43. Poser I, Sarov M, Hutchins JR, et al. BAC TransgeneOmics: a high-throughput method for exploration of protein function in mammals. *Nat Methods*. 2008;5:409–415.
44. Ionides A, Francis P, Berry V, et al. Clinical and genetic heterogeneity in autosomal dominant cataract. *Br J Ophthalmol*. 1999;83:802–808.
45. Shi Y, Bassnett S. Inducible gene expression in the lens using tamoxifen and a GFP reporter. *Exp Eye Res*. 2007;85:732–737.
46. Bassnett S. On the mechanism of organelle degradation in the vertebrate lens. *Exp Eye Res*. 2009;88:133–139.
47. Rodney S, Imarisio S. Developing a transgenic marker to research Huntington's disease in Drosophila melanogaster. *Int. J. Collab Res Int MedHealth*. 2010;2:199–213.
48. Seibel NM, Eljouni J, Nalaskowski MM, Hampe W. Nuclear localization of enhanced green fluorescent protein homomultimers. *Anal Biochem*. 2007;368:95–99.
49. Wei X, Henke VG, Strubing C, Brown EB, Clapham DE. Real-time imaging of nuclear permeation by EGFP in single intact cells. *Biophys J*. 2003;84:1317–1327.
50. Robinson ML, Overbeek PA. Differential expression of alpha A- and alpha B-crystallin during murine ocular development. *Invest Ophthalmol Vis Sci*. 1996;37:2276–2284.
51. Bhat SP. Crystallins, genes and cataract. *Prog Drug Res*. 2003; 60:205–262.
52. Horwitz J. Alpha-crystallin. *Exp Eye Res*. 2003;76:145–153.
53. Thomson JA, Augusteyn RC. Ontogeny of human lens crystallins. *Exp Eye Res*. 1985;40:393–410.
54. Mou L, Xu JY, Li W, et al. Identification of vimentin as a novel target of HSF4 in lens development and cataract by proteomic analysis. *Invest Ophthalmol Vis Sci*. 2010;51:396–404.
55. Gebhard S, Hattori T, Bauer E, et al. Specific expression of Cre recombinase in hypertrophic cartilage under the control of a BAC-Col10a1 promoter. *Matrix Biol*. 2008;27:693–699.
56. Gerfen CR, Paletzki R, Heintz N. GENSAT BAC cre-recombinase driver lines to study the functional organization of cerebral cortical and basal ganglia circuits. *Neuron*. 2013;80: 1368–1383.
57. Jaffe NS, Horwitz J. *Lens and Cataract. Textbook of Ophthalomology*. New York: Gower Medical Publishing; 1992.
58. Zhou L, Zhang Z, Zheng Y, et al. SKAP2, a novel target of HSF4b, associates with NCK2/F-actin at membrane ruffles and regulates actin reorganization in lens cell. *J Cell Mol Med*. 2011;15:783–795.
59. Guzman LM, Belin D, Carson MJ, Beckwith J. Tight regulation, modulation, and high-level expression by vectors containing the arabinose PBAD promoter. *J Bacteriol*. 1995;177:4121–4130.
60. Schmittgen TD, Livak KJ. Analyzing real-time PCR data by the comparative C(T) method. *Nat Protoc*. 2008;3:1101–1108.
61. Nishimoto S, Kawane K, Watanabe-Fukunaga R, et al. Nuclear cataract caused by a lack of DNA degradation in the mouse eye lens. *Nature*. 2003;424:1071–1074.
62. Cui X, Wang L, Zhang J, et al. HSF4 regulates DLAD expression and promotes lens de-nucleation. *Biochim Biophys Acta*. 2013;1832:1167–1172.

Investigative Ophthalmology & Visual Science